Int. J. Adhesion Adhesives. **23**, 437-448(2003).

Surface Energy, Surface Topography & Adhesion.

D.E. Packham
Centre for Materials Research,
University of Bath,
Claverton Down,
Bath, BA2 7AY

Abstract

In this paper are discussed some of the fundamental principles which are relevant to an understanding of the influence that interfacial roughness may have on adhesion. The surface energies of the adhesive, substrate and of the interface between them determine the extent of wetting or spreading at equilibrium. Numerical values for surface energies may be obtained either from contact angle measurements or from analysing force-displacement curves obtained from the surface forces apparatus. The extent to which the relationships, appropriate for plane surfaces, may be modified to take into account interfacial roughness are discussed. For modest extents of roughness, the application of a simple roughness factor may be satisfactory, but this is unrealistic for many of the practical surfaces of relevance to adhesive technology which are very rough, and is ultimately meaningless, if the surface is fractal in nature. Some examples are discussed of published work involving polymer-metal and polymer-polymer adhesion, where the roughness of the interface exerts a significant influence on the adhesion obtained. Roughness over a range of scales from microns to nanometres may strengthen an interface, increasing fracture energy by allowing bulk energy dissipating processes to be activated when the bond is stressed.

Keywords: B. Surface roughness/morphology; C. Contact angles; D. Adhesion by mechanical interlocking; Fractal surfaces; Surface forces apparatus

This paper is concerned to review some fundamental considerations which influence the effect of surface topography on the strength of an adhesive joint. The contact of a liquid adhesive with a rough solid surface is of obvious relevance to this subject. It is therefore necessary first to discuss basic concepts of surface energy and to develop the idea of surface roughness.

1. SURFACE ENERGY

1.1 Surface energy and adhesion

The basic concept of surface energy is that it is the excess energy associated with the presence of a surface. It is expressed *per unit area.* In formal treatments it is necessary to recognise that they may be defined in terms either of Gibbs G or Helmholtz F free energies. Distinction is also drawn between the 'surface energy' G^S and the surface tension γ [1,2]. In adhesion science and technology the interest is usually in complex solid surfaces for which very precise measurements of surface energy are not generally possible. It is therefore common, even universal, in this context to gloss over the formal distinctions between these terms and to take γ and G^S as being the same referring to both as 'surface energy'.

Considerations of surface energetics are usually regarded as fundamental to an understanding of adhesion. Surface energies are associated with *formation* of the adhesive

bond. A prerequisite for adhesion is contact between the phases 1 and 2 forming the bond. Commonly the adhesive is applied as a liquid, and its angle of contact θ with the solid is related to the surface energies by Young's equation [3]

$$\gamma_{1v} = \gamma_{12} + \gamma_{2v} \cos \theta \qquad (1)$$

where v refers to the vapour in equilibrium with the solid(1) and liquid(2).

The energy change (per unit area) when liquid 2 spreads over the surface of solid 1 is called the spreading coefficient or spreading energy, S, [3] and is also related to the surface energies:

$$S = \gamma_{1v} - \gamma_{2v} - \gamma_{12} \qquad (2)$$

If S is positive, the liquid at equilibrium will be spread completely over the solid.

Surface energies are also associated with *failure* of an adhesive bond. Failure involves forming new surfaces and the appropriate surface energies have to be provided. The surface energy term may be the work of adhesion, W_A, or the work of cohesion, W_C, depending on whether the failure is adhesive or cohesive. These are defined as follows [3] :

$$W_A = \gamma_1 + \gamma_2 - \gamma_{12} \qquad (3)$$

$$W_C = 2\gamma_1 \qquad (4)$$

The practical adhesion, for example fracture energy G, will comprise a surface energy term G_0 (W_a or W_c) to which must be added a term ψ representing other energy absorbing processes - for example plastic deformation - which occur during fracture:

$$G = G_0 + \psi \qquad (5)$$

Usually ψ is very much larger than G_0. This is why practical fracture energies for adhesive joints are almost always orders of magnitude greater than works of adhesion or cohesion. However a modest increase in G_0 may result in a large increase in adhesion as ψ and W are usually coupled. For some mechanically simple systems where ψ is largely associated with viscoelastic loss, a multiplicative relation has been found:

$$G = G_0 \{1 + \phi(c,T)\} \approx G_0 \times \phi(c,T) \qquad (6)$$

where ϕ(c,T) is a temperature and rate dependent viscoelastic term [4, 5]. In simple terms, stronger bonds (increased G_0) may lead to much larger increases in fracture energy because they allow much more bulk energy dissipation (increased ψ) during fracture.

1.2 Surface energy measurement

Contact angles Before equations such as 3 and 4 can be used, values for the surface energies have to be obtained. While surface energies of liquids may be measured relatively easily by methods such as the du Nouy ring and Wilhelmy plate[6], those of solids present more problems. Many of the most widely used methods are based on measuring the contact angles of a series of test liquids on the solid surface, and evaluating the surface energies via Young's equation, equation 1 above.

The surface energy of the solid γ_s can be obtained from equilibrium contact angle measurements of a series of test liquids on the solid surface, providing the relationship between γ_{sl} and the solid γ_s (in vacuo) and liquid γ_{lv} surface energies is known. The exact relationship is given by the Good and Girifalco equation[7, 8]:

$$\gamma_{sl} = \gamma_s + \gamma_{lv} - 2\phi\sqrt{(\gamma_s \gamma_{lv})} \qquad (7)$$

$$\gamma_s - \gamma_{sv} = \pi_e \qquad (8)$$

where ϕ is the Good -Girifalco interaction parameter and π_e is called the spreading pressure. The spreading pressure is difficult to measure, and it is common to neglect it. This may be justifiable for a low energy, non-polar solid (e.g. an alkane), but is difficult to justify where a high surface energy solid is involved. In principle the solid surface energy is calculated by eliminating γ_{sl} between equations 1 and 7 giving:

$$\gamma_{lv}\,(1 + \cos\theta) = 2\phi\sqrt{(\gamma_s\,\gamma_{lv})} \qquad (9)$$

The difficulty with equation (9) is that ϕ is not generally known. Over past decades enormous intellectual effort has been put into devising ways of circumventing the problem of not knowing ϕ, and much controversy has been generated in the process. Three of the resulting relationships are

$$\gamma_{lv}\,(1 + \cos\theta) = 2\sqrt{(\gamma_s^{\,d}\,\gamma_{lv}^{\,d})} + 2\sqrt{(\gamma_s^{\,p}\,\gamma_{lv}^{\,p})} \qquad (10)$$

proposed by Owens and Wendt [9], Kaelble and Uy[10],

$$\gamma_{lv}\,(1 + \cos\theta) = 4(\gamma_s^{\,d}\,\gamma_{lv}^{\,d})/(\gamma_s^{\,d} + \gamma_{lv}^{\,d}) + 4(\gamma_s^{\,p}\,\gamma_{lv}^{\,p})/(\gamma_s^{\,p} + \gamma_{lv}^{\,p}) \qquad (11)$$

proposed by Wu[11] and

$$\gamma_{lv}\,(1 + \cos\theta) = 2\sqrt{(\gamma_s^{\,LW}\,\gamma_{lv}^{\,LW})} + 2\sqrt{(\gamma_s^{\,+}\,\gamma_{lv}^{\,-})} + 2\sqrt{(\gamma_s^{\,-}\,\gamma_{lv}^{\,+})} \qquad (12)$$

due to Good [12]. All imply that the spreading pressure may be neglected.

These equations result from assuming that the total surface energy can be split into the sum of components associated with different types of bonding, for example dispersion γ^d plus polar γ^p (equations 10 and 11), or Lifshitz-van der Waals γ^{LW} plus acid-base γ^{AB} (equation 12). The γ^+ and γ^- terms are respectively the Lewis acid and Lewis base component of surface interaction: these are related to the acid-base component γ^{AB} by

$$\gamma^{AB} = 2\sqrt{(\gamma^+\,\gamma^-)} \qquad (13)$$

Surface forces apparatus An alternative approach to measuring surface energies is provided by the surface forces apparatus [13]. The apparatus uses crossed cylinders of molecularly smooth cleaved mica between which forces may be measured with a sensitivity of 10^{-8} N (10^{-6} gf). (The crossed cylinder configuration is locally equivalent to a sphere near a flat surface or to two close spheres [13]).The basic experiment by which surface forces apparatus is used to deduce surface energy values involves bringing the two surfaces concerned into contact and observing either the load necessary to cause them to separate, or the relationship between the radius of the contact zone and the applied load.

The results are most commonly analysed by the Johnson, Kendall and Roberts (JKR) equation [14]. For two elastic spheres, of radii R_1 and R_2, in contact this takes the form:

$$a^3 = [F + 3\pi R W_{12} + \sqrt{\{6\pi R\, W_{12}\, F + (3\pi R\, W_{12})^2\}}]R/K \qquad (14)$$

where

a is the radius of the area of contact,

$R = R_1\,R_2/(R_1 + R_2)$,

F is the normal load,

K is an elastic constant.

The term W_{12} is a surface energy term which is obtained via equation 14 from a plot of a^3 vs. load F. If we may assume that the spreading pressure is zero (equation 8), the surface energy term W_{12} will be the work of adhesion (equation 3) where surfaces 1 and 2 are different, and work of cohesion (equation 4) where they are the same.

An issue, at present unresolved, is that Derjaguin, Muller and Toporov [15, 16] have put forward a different analysis of the contact mechanics from JKR. Maugis has described a theory which comprehends both the theories as special cases [17].

2. SURFACE TOPOGRAPHY

2.1 Roughness factor

We have seen both how the concept of surface energy in principle relates to adhesion, and have examined some methods by which it may be measured. The surface energy terms discussed (e.g. equations 1 to 6) are all energies *per unit area.*

If the interface between phases 1 and 2 is 'perfectly' flat, there is no problem in defining the interfacial area, A. However most of the surfaces we work with are to a degree rough. If the roughness is not very great it might be adequately expressed by a simple Wenzel roughness factor[18],

$$r = A/A_o \qquad (15)$$

where A is the 'true' surface area, A_o the nominal area. For simple ideal surfaces, r can be calculated from elementary geometric formulæ. Thus a surface consisting of equal hemispheres would have a roughness factor of 2, one consisting of square pyramids with all sides of equal length, a roughness factor of $\sqrt{3}$. For simple real surfaces the roughness factor can be calculated from straight forward measurements, such as profilometry. In such cases we could substitute a corrected area into the definition of surface energy and thence via equation 3 evaluate work of adhesion. This approach assumes that there are no differences between the chemical nature and environment of surface molecules on the rough surface and on the smooth one.

2.2 Further conceptual development

Can the simple roughness factor approach (equation 15) be applied if the surface is very much rougher? Many of the surfaces encountered in adhesion technology are very rough indeed. Figure 1(a) shows a phosphated steel surface prepared for rubber bonding [19], figure 1(b) surface treated P.T.F.E [20]. As the scale of roughness becomes finer, the application of a simple roughness factor becomes increasingly unrealistic and unconvincing. It becomes unconvincing not just because of increasing practical difficulty in measuring the 'true' area of such surfaces, it becomes conceptually unconvincing. The roughness itself is an essential characteristic of the surfaces. As we approach molecular scale roughness, indeed long before we get there, the energy of the surface molecules is a consequence of the topological configurations they take up. It is unjustifiable to regard these surfaces as essentially the same as smooth surfaces which happen to be rough!

Figure 1
Examples of rough pretreated substrate surfaces.
(a) Phosphated steel prepared for rubber bonding [cf. 19]
(b) P.T.F.E. irradiated by argon ions [20].

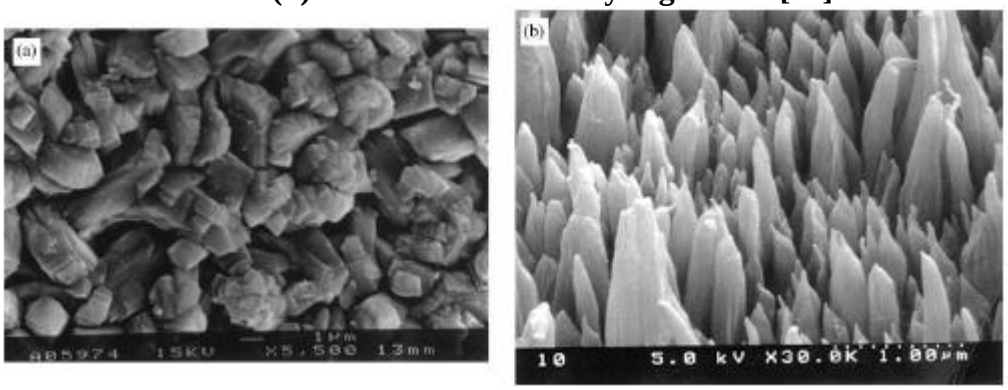

Further, roughness at an interface may actually develop as a result of bringing the two phases together. They will take up these configurations as a consequence of the molecular interactions at the interface: they are an essential feature of bringing together the two phases 1 and 2. Such roughening can be seen as an increasing of the low surface entropy implied by a smooth surface [15, 21-23].

Fractal surfaces It has long been recognised from work on gas adsorption on porous solids that the surface area measured depends on the size of the probe molecule [24], and is therefore in a sense arbitrary, not absolute. More recently the development of the mathematics of fractals has brought into clear focus the dependence of the area of a rough surface on the size of the 'tile' used to measure it, the actual relationship depending on the fractal dimension of the surface. The area of such a surface tends to infinity as the tile size tends to zero. (An introduction to the concept of fractals may be found in reference 25.)

2.3Roughness factor for a fractal surface

Consider the adsorption of probe molecules of various sizes (*cross-sectional area σ) on a fractal surface [25, 26]. Let n be the number of molecules required to form a monolayer. If log n(σ) is plotted against log σ, a straight line with negative slope is obtained which can be represented as

$$\log n(\sigma) = (-D/2).\log \sigma + C \qquad (16)$$

where D is the fractal dimension of the surface (C and C', k, β, β' and β" below are constants).

$$\therefore\ n(\sigma) = \beta.\sigma^{-D/2} \qquad (17)$$

The area
$$A = n(\sigma).\sigma \qquad (18)$$

$$\therefore\ A(\sigma) = \beta.\sigma^{1-D/2} \qquad (19)$$

This can be expressed in terms of a *linear dimension λ.

$$\text{Now } \sigma = k\,\lambda^2 \qquad (20)$$

$$\therefore\ \log n(\lambda) = (-D/2).\log k\,\lambda^2 + C \qquad (21)$$

$$= -D \log \lambda + C' \qquad (22)$$

$$\therefore\ n(\lambda) = \beta'\,\lambda^{-D} \qquad (23)$$

and
$$A(\sigma) = n(\lambda).\sigma = n(\lambda).k\,\lambda^2 \qquad (24)$$

$$= k\,\lambda^2\,\beta'\,\lambda^{-D} \qquad (25)$$

$$\therefore\ A(\sigma) = \beta''\,\lambda^{2-D} \qquad (26)$$

Consider the roughness factor, r, for such a fractal surface

$$r = A/A_o \qquad (15)$$

where A is the 'true' surface area, A_o the nominal area, i.e. the area of a plane surface. For a plane surface D = 2, so

$$r = A/A_o = \beta''\,\lambda^{2-D}/\beta'' = \lambda^{2-D} \qquad (27)$$

for a fractal surface D>2, and usually D<3. In simple terms the larger D, the rougher the surface. The intuitive concept of surface area has no meaning when applied to a fractal surface. An 'area' can be computed, but its value depends on both the fractal dimension and the size of the probe used to measure it. The area of such a surface tends to infinity, as the probe size tends to zero.

Obviously the roughness factor is similarly arbitrary, but it is of interest to use equation 27 to compute its value for some trial values of D and λ. This is done in Table 1. In order to map the surface features even crudely, the probe needs to be small. It can be seen that high apparent roughness factors are readily obtained once the fractal dimension exceeds two, its value for an ideal plane.

* Note. Both σ and λ must be in dimensionless form, as a ratio to some large, fixed area or length such as sample area or length.

Table 1 'Roughness factor' calculated for a fractal surface, according to the fractal dimension D and probe length λ.

D	Roughness factor for values of λ as indicated:			
	$\lambda = 10^{-2}$	10^{-4}	10^{-6}	10^{-9}
2	1	1	1	1
2.1	1.6	2.5	4	7.9
2.5	10	100	1000	32000
2.8	40	1600	63000	16000000

While not wishing to question the value of the roughness factor concept for taking into account modest departures from the flatness of a surface, I would suggest that it is not meaningful to talk of *the* area a rough surface as if it had in principle an unique value. It seems inescapable, then, that when we refer to the surface area A in the context of surface energy and work of adhesion (equations 1 to 6) we must use the ideal, formal area, i.e. macroscopic area of the interface. This has important implications for the effect of surface roughness on adhesive joint strength.

3. SURFACE ROUGHNESS AND WETTING

3.1 Effect on contact angle

Young's equation 1 may be derived by considering the small displacement from equilibrium of a sessile drop on a plane surface and making the rate of change of energy with position zero [6]. If the same derivation is applied to the situation where the solid surface has a roughness factor (equation 15) of r [18], it is readily seen that

$$\cos \theta_{rough} = r \cos \theta_{smooth} \qquad (28)$$

This much-quoted equation immediately suggests that

$$\text{if } \theta_{smooth} < \pi/2 \quad \text{then} \quad \theta_{rough} < \theta_{smooth}$$
$$\text{but if } \theta_{smooth} > \pi/2 \quad \text{then} \quad \theta_{rough} > \theta_{smooth}$$

This glosses over the problem that the observed contact angle on a surface is related to an assumed horizontal, but one might expect on a microscopic level that with a rough surface the liquid would take up an equilibrium value (θ_{smooth}) with the gradient of the surface at the edge of the drop.

The effect of Wenzel roughness on the spreading of liquid 2 on solid 1 is perhaps better examined using the concept of the spreading coefficient. With a roughness factor of r, equation 2 may be rewritten as

$$S/\gamma_2 = r.(\gamma_{1v} - \gamma_{12})/\gamma_2 - 1 \qquad (29)$$

This predicts that if $\gamma_{1v} - \gamma_{12}$ is positive ($\theta_{smooth} < \pi/2$), roughening will enhance the tendency for spreading to occur, but if $\gamma_{1v} - \gamma_{12}$ is negative ($\theta_{smooth} > \pi/2$), it will reduce this tendency [27].

It is important to be clear about the assumptions on which equations 28 and 29 are based. It is assumed that roughening has no effect on the atomic arrangement of the solid: the limitations of this were discussed in section 2.2 above. A further assumption is that, within the drop of liquid, the liquid is able to come into perfect contact with the solid without entrapping air, however high the contact angle.

Cassie [28] extended Wenzel's treatment to composite surfaces, such as rough surfaces incompletely wetted by a liquid. If an area fraction f_1 is wetted and f_2 unwetted surface,

$$\cos \theta_{rough} = r f_1 \cos \theta_{smooth} - f_2 \qquad (30)$$

where r is the roughness factor. $\theta_{rough} > \theta_{smooth}$ unless the roughness factor is relatively large. The two contact angles are obviously equal where

$$\cos \theta = f_2 /(r f_1 - 1) \qquad (31)$$

If the contact angle is known, it possible to calculate the extent of wetting for idealised rough surfaces. It is necessary to consider whether these conclusions require modification in the light of kinetic effects, such as setting of the adhesive.

3.2 Equilibrium Considerations

The extent of contact between a liquid and a rough surface depends on the details of the topography. For example, penetration into an idealised pore, as shown in Figure 2 [29, 30], occurs until the back pressure of trapped air equals the capillary driving pressure. De Bruyne showed that the capillary driving pressure for such a pore was given by

$$2 \gamma_2 \sin(\theta + \phi)/(r_o - x.\cot \phi) \qquad (32)$$

The symbols are defined on Figure 2. If $(\theta + \phi)$ is less than 180°, some penetration will occur. Greater wetting of the pore is favoured by low contact angle and low ϕ. For a cylindrical pore ($\phi = 90°$), the distance x penetrated into a pore of length ℓ and radius r is

$$x = \ell . (1 - \{P_a r/[2 \gamma_2 \cos\theta + P_a r]\}) \qquad (33)$$

where P_a is atmospheric pressure. Clearly the smaller the pore the greater the proportion of its length filled at equilibrium. Under many circumstances adhesive-substrate contact will be less than that predicted by the Wenzel approach, equations 28 and 29.

Figure 2
Section through an idealised pore [after 29]

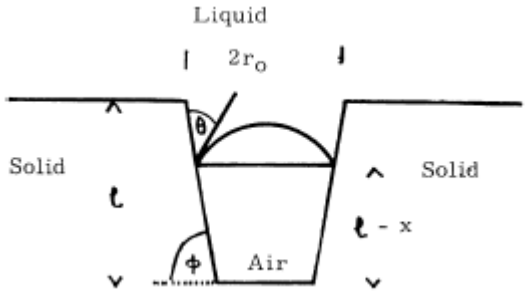

These discussions assume that equilibrium contact between liquid adhesive and rough substrate is achieved. However adhesives set in what may be quite a short time, and so may never reach equilibrium contact [30, 31].

Although much of the discussion above of pore penetration is in terms of empirical or simplified relationships it does serve to give an indication of the influence of relevant factors on the wetting of a rough surface by a polymeric adhesive. Roughness may seriously limit the extent of contact, but this is not necessarily so. Under favourable circumstances good penetration of the adhesive should be achieved into the topographical features of the substrate surface.

4. SURFACE ROUGHNESS AND JOINT STRENGTH

The roughness of an interface may be on any scale ranging from the macro to the molecular. It can affect joint strength in a number of different ways. Some examples, illustrating them will be presented, broadly moving from large scale roughness to roughness at a nano level.

4.1 Some effects observable on a large-scale.

Roughness factor For moderately rough surfaces, an increase in surface area may well lead to a proportionate increase in adhesion, so long as the roughness does not reduce contact between the surfaces [32]. Gent and Lai have convincingly demonstrated the effect in careful experiments with rubber adhesion. In comparing adhesion to smooth and to grit blasted steel, they observed increases in peel energy by factors of 2 to 3 times which they ascribed to the increase in surface area.

Simple key. Some ingenuity has been used to produce surfaces with a classic 'key' A conceptually simple example of this is the adhesion of silica to copper discussed by van der Putten [33], who was concerned to bond copper directly to silica in the context of integrated circuit technology.

Copper sticks poorly to silica but titanium tungstide sticks well. Using conventional lithographic techniques islands of TiW 0.1 μm thick were sputtered onto the silica and the photoresist was removed (figure 3(a)).

Palladium acts as a nucleating agent for the electroless deposition of copper. By treating the surface with palladium [II] chloride in hydrochloric acid a monolayer or so of palladium is deposited on the TiW surface. The palladium chloride solution also contains 1% of hydrofluoric acid which attacks the silica, undercutting the TiW islands (figure 3(b)). Electroless copper is now deposited, nucleating on the palladium covered TiW and growing from it. Finally copper is electrodeposited and is thus mechanically anchored to the silicon surface (figure 3(c) and (d)).

Here the stress is directed away from the low W_a interface (silica/copper) towards the stronger silica / palladium interface by the topography produced. The surface topography protects weak regions from a high stress field.

Figure 3
Adhesion of silica to copper using a mechanical key [after 33]

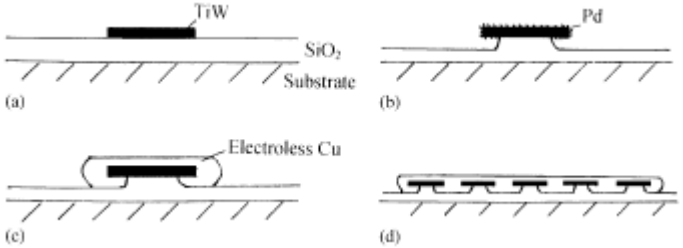

In some literature reports adhesion between sheets of semi-crystalline polymers, such as polypropylene and polyethylene, where a laminate has been formed by cooling from the melt, the lower-melting polymer has been shown to flow into the structure of the higher-melting material as its volume contracts on crystallisation [34-37]. These influxes, which may be hundreds of microns in size, lead to a mechanically-reinforced interface. On peeling the laminates the influxes lead to enhanced plastic deformation in the interfacial regions and so to enhanced adhesion (cf. equation 5).

Elastic and plastic losses.

Gent and Lin have shown that large amounts of energy can also be involved in peeling an *elastic* material from a rough surface[38]. The energy is essentially used for the elastic deformation of embedded filaments: this energy is lost because when the filaments become free, they immediately relax.

Gent and Lin experimented with rubber bonded to aluminium plates with regular arrays of cylindrical holes. The peel energy was low for the plates in the absence of holes. An energy balance analysis gives the ratio of fracture energy for peeling from the material with cylindrical pores G_a' to that from a smooth substrate G_a as

$$G_a' / G_a = 1 + 4 \phi l /a \qquad (34)$$

where l is the pore length, a its radius and ϕ the ratio of pore area to total area of the plate[38]. Their experimental results demonstrated the essential validity of this relationship. Where pull-out alone occurred the work of detachment for their system increased by up to 20 times.

They further considered the situation where fracture of strands occurred. The extra work is proportional to depth of pores and for their system could be several hundred times the work of detachment from a smooth surface. This energy term dominates for deep pores.

Most polymers used as adhesives or coatings will not act as perfect elastic bodies uniformly stressed up to fracture. Uneven stress distributions and plastic yielding would be expected to increase the energy dissipation observed beyond that calculated for the ideal elastic model.

While calculations like those discussed involve serious simplifications and idealisations, they do serve to show that surface roughness *per se* is capable of increasing the fracture energy of an adhesive joint by a large amount. Gent and Lin's model clearly represents many practical adhesive systems where adhesion to microfibrous or microporous substrates, such as anodised aluminium are involved [39].

It will be very interesting to see whether auxetic materials (materials with a negative Poisson's ratio) can be developed to an extent that they can be used as coatings for such porous substrates. Considerable increases in fracture energy can be anticipated.

4.2 Cognate chemical change.

It is certainly very difficult, if not impossible, to change the topography of a surface without altering its chemical nature in some way. There are many reports both of mechanical effects supplementing chemical ones and opposing their influence. Two illustrative papers are discussed.

Zhuang and Wightman [40] studied both the surface topography and the surface chemistry of carbon fibres modified by treatment with an oxygen plasma prior to incorporating into an epoxy matrix. Two types of fibres, differing in surface roughness, were studied. An increase in surface oxygen content was observed on treatment, mirrored by increase in polar component of surface energy and in interfacial shear strength, IFSS. Here the rougher fibres had somewhat lower IFSS. The lower adhesion was associated with incomplete filling by the resin of valleys on the fibre surface striations. However there is evidence that the rougher surface imparts better durability in a humid environment.

P.T.F.E. is a notoriously difficult substrate to bond. Koh et al. [20] have used argon ion irradiation as a pretreatment both in the presence and absence of oxygen. The treatment produced increasing roughness, eventually giving a fibrous forest-like texture, (figure 1(b)). Adhesion to the treated surfaces was studied in several different ways, and generally considerable enhancement was found, which appeared to peak at a treatment level of 10^{16} ions /cm^2. (figure 4).

High-resolution XPS spectra showed the chemical changes occurring. In the absence of oxygen, a 285 eV (C-C and C-H) peak developed with maximum intensity at a dose of 10^{16} ions /cm^2. In the presence of oxygen a strong O1s signal developed which was attributed to the reaction of oxygen atoms with the free radicals created by argon ion bombardment. The authors attribute the enhanced adhesion to a combination of improved wettability and chemical reactivity of the surface, combined with mechanical keying to the

increasingly rough surfaces. There is no convincing explanation of the fall in adhesion at the highest treatment time. It would be interesting to know at what level the difference between adhesion at 10^{16} and 10^{17} ions /cm^2 was statistically significant.

Figure 4
Surface treatment of P.T.F.E. by argon ion irradiation: variation of adhesion with ion dose [20].

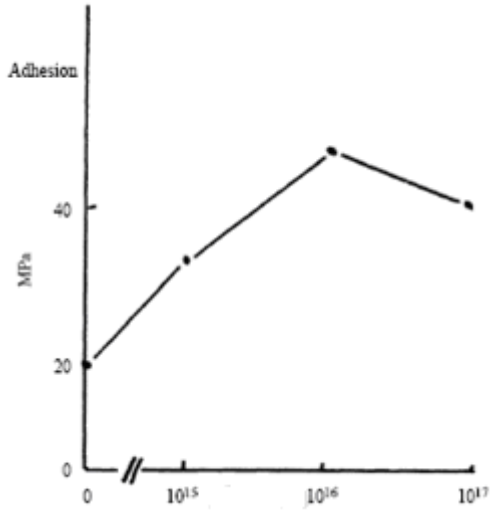

4.3 Fractal results

Grit-blasting is a well-established and widely-used stage in the pretreatment of metal surfaces. Despite sporadically investigation over many decades, no general view has emerged of how the characteristics of the surface influence the adhesion [41, 42]. In a recent investigation, Amada et al. [43, 44] grit blast a steel substrate, varying the angle between the gun and the specimen surface, and measured the adhesion of a plasma-sprayed alumina coating. They examined profiles of the grit-blasted surfaces and argued that their form was that of a self-affine fractal, the dimension of which depended on the blasting angle. The highest fractal dimension (1.07) is reported to correspond with the blasting angle which gave maximum adhesion. The fractal dimension correlated better with adhesion than did surface roughness measurements.

The deposition of metal coatings on polymers provided some well-characterised examples where mechanical effects were significant in adhesion, and played a rôle in the re-establishment of the mechanical theory of adhesion in the early seventies [30, 45]. In these examples, a polymer, such as A.B.S. was etched to remove one phase from the surface regions, leaving micron-scale pits which acted as a key for the deposited metal. More recently Mazur et al. [46] electrodeposited silver within a polyimide film under conditions where the silver(I) solution was able to diffuse into the polymer film where it was reduced to the metal. The adhesion was excellent: the only way that Mazur could remove the silver was by abrasion.

Examination of a section through the interface by transmission electron microscopy shows an extremely rough interfacial region on sub-micron scale. Wool et al. [47] analysed the profile and showed the interface to be fractal with a dimension of around 1.6.

4.5 Polymer-polymer adhesion

Microscale Janarthanan et al. [48] have employed roughness on a micron scale to enhance the adhesion between two immiscible polymers, polycarbonate and styrene-acrylonitrile copolymer, SAN. Grooves of depths between 5 and 35 μm were scribed in the

polycarbonate surface before laminating the two polymers by hot pressing. The fracture toughness of the laminate, which was determined using a double cantilever beam test specimen, increased from 8 J/m^2 for the ungrooved specimen to 170 J/m^2 for the specimen with 35 μm grooves. The crack propagated by a stick-slip mechanism, slowing considerably at each groove. The increased toughness was associated with extensive deformation of both polymers in the vicinity of the grooves.

Adhesion of thermodynamically incompatible polymers is of current interest because of its implications for developing new multiphase polymer materials and for recycling of mixed plastic wastes. Many elegant experiments have been reported in which the interfacial structure has been investigated, often in the present of various types of copolymer added at the interface as putative compatibilisers.

Hashimoto et al. [21] annealed the interface between polystyrene and a styrene-isoprene diblock polymer at 150 °C and showed extensive roughening of the interface by mutual interdiffusion.

Delevopment roughness on a nano-scale Creton et al. [23] studied the adhesion of a somewhat similar system using a surface forces-type apparatus. Contact was made between a crosslinked polyisoprene hemisphere and a thin polystyrene sheet. The fracture energy was comparable in magnitude (although not numerically close) to the work of adhesion 0.065 J/m^2. When the polystyrene surface was covered with a layer of a styrene-isoprene diblock polymer considerably higher adhesion was observed which increased with crack speed. G_0, the limiting value at zero crack speed increased with both surface density (Σ) and degree of polymerisation (N_{PI}) of the polyisoprene chains (Figure 5). While the blurring of the interface is on a much more limited scale that shown by Hashimoto, Creton et al. argue that the isoprene end of the diblock copolymer molecules diffuses into the crosslinked polyisoprene, and that the additional fracture energy is associated with the frictional drag as these chains are pulled out under influence of the applied load.

Figure 5
Increase in threshold fracture energy, G_0,
with length (N_{PI}) and surface density (Σ)of isoprene chains [23].
Degree of polymerisation: (i) 558, (ii) 882 (iii) 2205

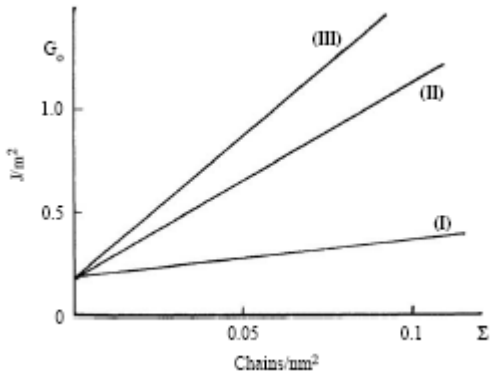

With suitable copolymers, roughening of the interface between two incompatible polymers by interdiffusion can lead to a range of values for fracture toughness G. For diblock copolymers both surface density (Σ) and degree of polymerisation (N) of the blocks are important. If the blocks are shorter than the entanglement length N_e of the corresponding homopolymer, failure occurs, as with the isoprene above, by chain pull-out and G is low. If $N > N_e$ chain scission will occur at low surface density (Σ), but as Σ is

increased the fracture energy G rises steeply and plastic deformation, for example crazing, occurs in the polymer followed by chain scission or pullout.

These effects have been found by Creton et al. [49] who laminated sheets of incompatible polymers, P.M.M.A. and P.P.O., and studied the adhesion using a double cantilever beam test to evaluate fracture toughness G_c . For the original laminate G_c was only 2 J/m^2, but when interface was reinforced with increasing amounts of a symmetrical P.M.M.A. - P.S. diblock copolymer of high degree of polymerisation ($N > N_e$), the fracture toughness increased to around 170 J/m^2, and then fell to a steady value of 70 J/m^2. (Figure 6). In some experiments the P.M.M.A. block was deuterated, in others the P.S. block. This enabled dynamic S.I.M.S. to be used to study the failure mode and elucidate the mechanism of adhesion. The ^{1}H and ^{2}H signals were normalised with respect to the ^{12}C signal.

At low surface coverage fracture occurs close to the junction point of the diblock, with each fragment remaining on the "correct" side of the interface. At higher values of Σ the surface saturates, crazing occurs during fracture and G_c reaches a maximum. With further increase in surface density of the copolymer a weak layer forms at the interface and the fracture toughness falls to a limiting value. Here S.I.M.S. suggests that some failure is still occurring at the diblock junction points, but increasingly in between multiple lamellae of the copolymer organised at the interface.

Figure 6
Adhesion of P.M.M.A. to P.P.O. Effect on fracture toughness, G_c, of interfacial density, Σ, of a reinforcing diblock copolymer [49].

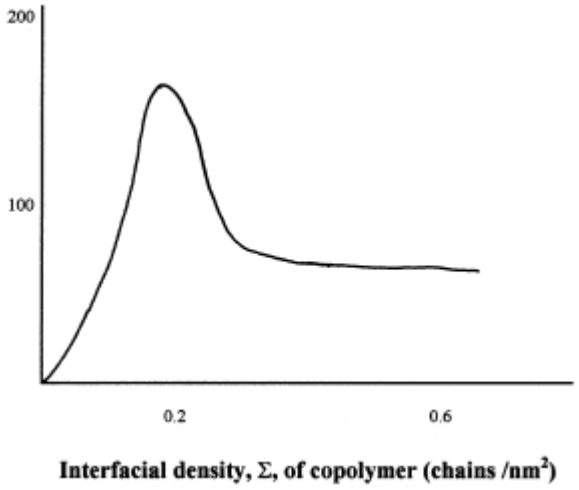

Results from the surface forces apparatus Results obtained with the surface forces apparatus throws some interesting light on the nature and roughness of surface layers in contact. If the contact between two similar layers is studied, equation 14 enables the surface energy to be evaluated. This can be calculated from results obtained both when the surfaces are advancing into closer contact, γ_A, and when they are receding further apart, γ_R. These two values would be expected to be the same, as indeed they some times are. In many cases however there is hysteresis with $\gamma_R > \gamma_A$. Israelachvili and his colleagues have studied this phenomenon in some detail [15, 50-52].

In a typical experiment, Israelachvili [15] deposited monolayers of surfactants onto cleaved mica sheets, and evaluated the surface energies using the JKR equation 14. Figure 7 contrasts results for mica coated with monolayers of (a) L-α-

dipalmitoylphosphatidylethanolamine (DMPE) where $\gamma_A = \gamma_R = 27 mJ/m^2$ and (b) hexadecyltrimethylammonium bromide (CTAB) where $\gamma_A = 20\ mJ/m^2$ and $\gamma_R = 50\ mJ/m^2$.

Figure 7
Use of the JKR equation (14) relating applied force, F, to radius of contact, a, to analyse results from the surface forces apparatus.
Surface energy, γ, of surfactant layers (DMPE) cf. (CTAB) [15].

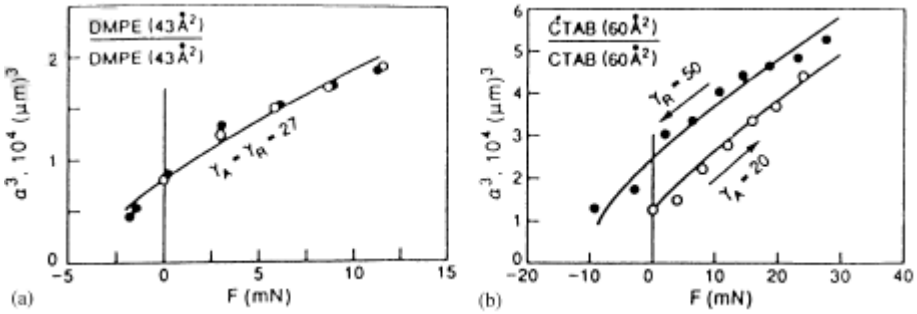

Figure 8
Schematic representation of solid-like (crystalline), amorphous solid, and liquid-like surface layers [50].

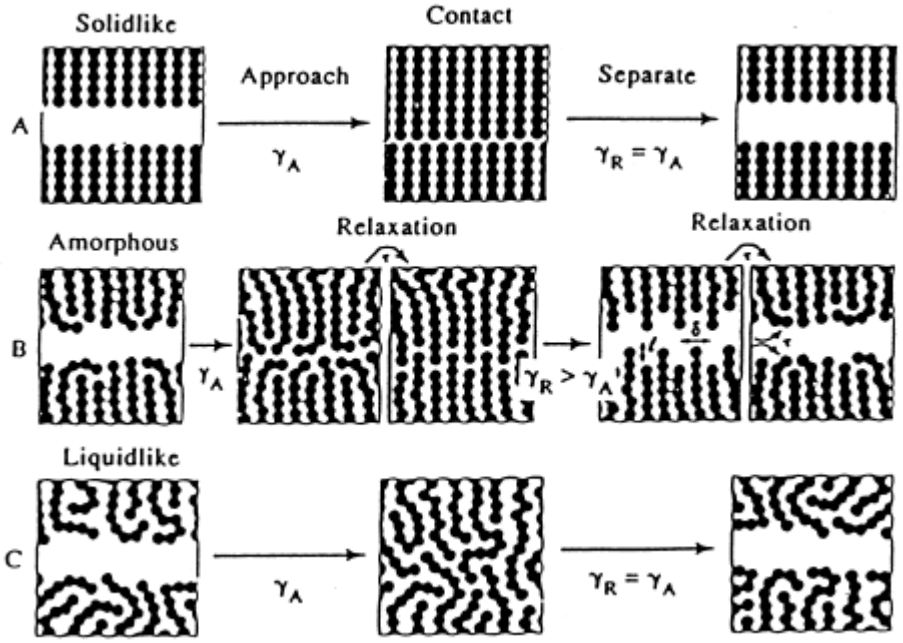

Israelachvili argues that the hysteresis is a result of reorganisation of the surface after they are brought into contact. This may occur at a macroscopic, microscopic or molecular level. Here he argues that interdigitation or interpenetration occurs, roughening the interface at the molecular level. He has classified his surface layers as crystalline (solid-like), amorphous solid and liquid-like (figure 8). The first tend not to reorganise, so hysteresis is low. The liquid-like surfaces reorganise very quickly both on loading and unloading, so again hysteresis tends to be low. It is the solid amorphous surfaces, where reorganisation may take place over a significant time scale, that hysteresis is generally greatest. On a simplistic level, the analogy with viscoelastic loss is obvious, and it is not surprising to find that adhesional hysteresis is considered to have a temperature / rate

dependence, figure 9. Under the experimental conditions employed DMPE forms a crystalline ordered layer, but the CTAB layer is amorphous.

Figure 9
Effect of temperature on adhesion hysteresis [52]

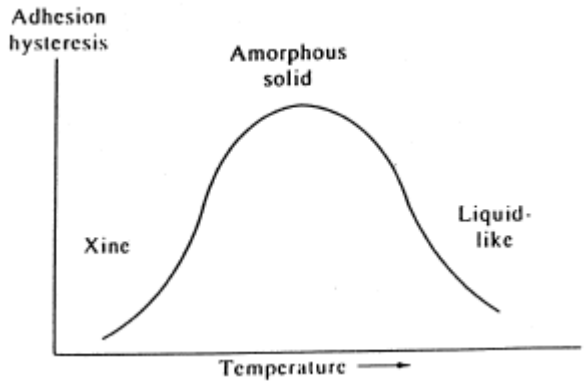

Thus this adhesion hysteresis is a result of a time dependent-roughening of the interface resulting from the intrinsic properties of the surface molecules. Israelachvili even interprets it in terms of a roughness factor effect (cf. equation 15), arguing that if $\gamma_R \approx 2\gamma_A$ then the true contact area has become about twice the nominal area of contact. It would seem more realistic to argue that the energy loss, associated with the hysteresis is related to the frictional forces involved in disentangling the rough, interdigitated surfaces.

Israelachvili has shown [15] that the kind of factors that lead to adhesion hysteresis can also lead to contact angle hysteresis. Reorganisation of the surface in contact with the test liquid may cause the receding angle to be grater than the advancing one.

5. DISCUSSION

Why does surface roughness affect adhesion? More particularly, why does increasing interfacial roughness often increase adhesion? In a simple way, we can rationalise this in terms of equation 5. Let us examine each term in turn, considering how it might contribute to the *hypothetical* fracture energy G of the adhesive joint.

$$G = G_0 + \psi \qquad (5)$$

The ***surface energy term G_0*** is of the form "surface excess energy" per unit area of surface, so may be expressed as

$$G_0 = \Delta G/A \qquad (35)$$

It is readily appreciated that surface treatments may increase ΔG by introducing more chemically active groups into the substrate surface. This is a central idea in the adsorption theory of adhesion. ΔG may also be increased as a result of roughening the surface. An atom near an asperity peak or fine fractal feature will clearly have a much greater 'atomic' surface energy, than a chemically similar atom in a plane crystal surface.

Turning attention to ***the area A*** in equation 35, it is important to remember that A refers to the formal area, the macroscopic area of the interface. For a rough surface the 'true' area will be greater. As we move from macroroughness towards roughness on a nano- and molecular scale, we move from the historic realm of the mechanical theory into the realm of the diffusion theory, at the same time the effective increase in A becomes enormous. Consequently G_0 may be raised to very high value. Indeed, as many engineering surfaces are fractal in nature [53], we can only retain the concept of 'area' at all, if we accept that it can be considered as indefinitely large. The practical adhesion does not

become infinite because the joint will fail (cohesively) in some other region where G_0 is smaller.

Returning to equation 5, consider the ***other energy absorbing processes*** ψ which occur during fracture. As we have seen these may include energy involved in chain pull-out or scission, and more generally plastic and elastic losses. Asperities and surface pits may alter the stress distribution at the interface so as to involve a larger volume of material in plastic deformation during fracture [54]. A consequence of roughening a surface will often be to increase these losses considerably, because they are coupled to the surface energy term G_0 (cf. equation 6).

Rough fracture surfaces It is significant that the fracture surfaces produced when strong adhesive bonds are broken are often extremely rough. (This, of course, holds for strong bonds irrespective of the roughness of the substrate surface.) Consider equation 5 which gives the fracture energy in terms of the terms which contribute to it. For the sake of being specific, suppose the failure mode is cohesive. Should the surface energy term be W_c, given by equation 4? This would not take into account the very rough surfaces produced in the fracture. The surface energy term needs to be increased by two factors, the first, r, taking into account the larger surface area, the second, s, allowing for the increased 'atomic' surface energy on the rough surface:

$$W^*_c = 2rs\,\gamma = W_c + (2rs - 2)\gamma \qquad (36)$$

If the roughness of the fracture surface is large this becomes

$$W^*_c = 2rs\,\gamma = W_c + 2rs\gamma \qquad (37)$$

and equation 5 is now

$$G = G_0 + 2rs\gamma + \psi \qquad (38)$$

The term r might be the roughness factor, but as argued above, it should often be a factor involving the fractal dimension of the fracture surfaces, which, as Table 1 shows, may be extremely large.

$$G = G_0 + 2s\gamma\,\lambda^{2-D} + \psi \qquad (39)$$

Mecholsky [55] has proposed an equation of this sort to represent the brittle fracture of ceramics.

6. CONCLUSIONS

The mechanical theory of adhesion is associated with adhesion to rough and porous surfaces. It is valuable in so far as it concentrates attention on surface roughness and the influence this may have on adhesion. Surface roughness of interest may range in scale from hundreds of microns to nanometres. Adhesion to rough surfaces may be effective because of the intrinsically high surface energy of atoms on an asperity surface. The increase in surface area, possibly by a very high factor, also raises the surface energy when expressed per unit nominal area.

Rough surfaces, when stressed, may be able to redistribute the stress so as to increase energy dissipation during failure of the joint. The strengthening of an interface resulting from increasing roughness may change the mechanism of fracture from a less to a more energetic mode. With increasing interfacial roughness between two incompatible polymers the mechanism may change from chain pull-out to crazing or other forms of plastic deformation.

It has been common for many years to rationalise adhesion phenomena in terms of a number of different theories of adhesion. While accepting that reductionism has been an extremely fruitful methodology in science, especially physical science, we should not forget that it *is* a methodological device and beware of accepting its categories too lightly

as having objective reality. In surveying the effect of roughness on adhesion, we can see how the concepts of adsorption diffusion and mechanical theories merge seamlessly in providing a model of the empirical observations.

REFERENCES

[1] Lewis G.N. and Randall M., Thermodynamics, 2nd edn. revised by K.S. Pitzer and L. Brewer, McGraw-Hill, 1961, p. 472.
[2] Somorjai, G.A. Principles of Surface Chemistry, Prentice-Hall, 1972.
[3] Padday J.F. in *Handbook of Adhesion,* ed. D.E. Packham, Longman 1992, p. 82
[4] Gent A.N. and Kinloch A.J., J. Polym. Sci. A2 1971; **9:** 659.
[5] Andrews E.H. and. Kinloch A.J., Proc. Roy. Soc. A 1973; **332:** 385 and 401.
[6] Adamson, A.W., *Physical Chemistry of Surfaces,* Wiley, 5th edn., 1990.
[7] Girifalco L.A. and Good R.J., J. Phys. Chem. 1957; **61:** 904.
[8] Girifalco L.A. and Good R.J., J. Phys. Chem. 1960; **64:** 561.
[9] Owens D.K. and Wendt R.C., *J. Appl. Polym. Sci.* 1969; **13:** 1741.
[10] Kaelble D.H. and Uy K.C. *J. Adhesion* 1970; **2:** 50.
[11] Wu S., J. Adhesion 1973; 5:39.
[12] Good R.J. and van Oss C.J., in *Modern approaches to wettability,* ed. M.E. Schrader and G.I. Loeb, Plenum, New York, 1992, p.12.
[13] Israelachvili J.N., Intermolecular and surface forces, 2nd edn. Academic Press, 1992.
[14] Johnson, K.L..Kendall K and Roberts A.D., Proc. Roy. Soc. 1971; A **324:** 301.
[15] Chen Y.L.,. Helm C.A and Israelachvili J.N., J. Phys. Chem. 1991; **95**: 10736.
[16] Derjaguin B.V., Muller V.M. and Toporov Yu P., J. Coll. Interf. Sci. 1975; **53**: 314.
[17] Maugis, D. J. Coll. Interf. Sci. 1992; **150**: 243.
[18] Wenzel R.N., Ind. Eng. Chem 1936; **28:** 988.
[19] Cook J. W., Edge S. and Packham D. E., *J. Adhesion* 2000;**72**: 293-316.
[20] Koh SK, Park SC, Kim SR, Choi WK, Jung HJ, Pae KD, Journal of Applied Polymer Science, 1997; **64:**1913.
[21] Koizumi, S. Hasegawa H. and Hashimoto T., Macromol. 1990; **24:** 2467.
[22] Wool R.P., *Polymer interfaces: structure and strength*, Munich Hanser, 1995, p. 129.
[23] Creton C., Brown H.R. and Shull K.R., Macromol. 1994; **27:** 3174.
[24] Rideal E.K. *Introduction to surface chemistry* 1930, p 175-6, 179, CUP.
[25] Harrison, A. Fractals in Chemistry, OUP, 1995, p. 6.
[26] Farin D. and Avnir D., in Fractal approach to heterogeneous chemistry, ed. D. Avnir, Wiley, 1989, p. 272.
[27] Padday J.F. in *Handbook of Adhesion,* ed. D.E. Packham, Longman 1992, p. 509.
[28] Cassie A.B.D., Disc Faraday Soc, 1948; **3:** 11.
[29] de Bruyne N.A., Aero Research Tech. Notes Bull. no. 168, Dec. 1956.
[30] Packham D.E. The adhesion of polymers to metals the role of surface topography, in Adhesion Aspects of Polymeric Coatings, ed. K.L. Mittal, Plenum, 1983, p.19.
[31] Shanahan, MER, in *Handbook of Adhesion,* ed. D.E. Packham, Longman 1992, p. 512.
[32] Gent A.N. and. Lai S.M, Rubber Chem. Technol. 1995; **68**: 13.
[33] van der Putten A.M.T., J. Electrochem. Soc. 1993; **140:** 2376.
[34] Yuan B-L and Wool R.P., Pol. Eng. Sci 1990; **30:** 1454.
[35] Wool R.P., *Polymer interfaces: structure and strength*, Munich Hanser, 1995, chapter 10, p.379.
[36] Bartczak Z. & Galeski A., Polymer 1986; **27:** 544.
[37] McEvoy R.L. & Krause S., Macromolecules, 1996; **29**: 4258.

[38] Gent A.N. and Lin C.W., J.Adhesion 1990; **32:** 113.
[39] Packham D.E., Mechanics of failure of adhesive bonds between metals and polyethylene and other polyolefins. *Developments in Adhesives - 2*, Applied Science Publishers, 1981, p.315.
[40] Zhuang, H and Wightman, JP, Journal of Adhesion, 1997; **62**: 213.
[41] Taylor D. and Rutzler J.E. Ind. Eng. Chem. 1958; **50:** 928.
[42] Harris AF, Beevers A, International Journal of Adhesion and Adhesives, 1999; 19: 445.
[43] Amada S, Satoh A, Journal of Adhesion Science and Technology, 2000; **14:** 27.
[44] Amada S, Hirose, T., Surf. Coatings Technology, 1998; **102:** 132.
[45] Packham D.E., in *1st International Congress on Adhesion Science and Technology: Invited papers* ed. W.J. van Ooij and H.R. Anderson, VSP Publishers, Utrecht, 1998, p. 81.
[46] Mazur, S. and Reich, S. J. Phys. Chem. 1986;90:1365.
[47] Wool R.P., *Polymer interfaces: structure and strength*, Munich Hanser, 1995, p. 132.
[48] Janarthanan V, Garrett PD, Stein RS, Srinivasarao M, Polymer, 1997; 38: 105.
[49] Creton C., Brown H.R. & Deline V.R., Macromolecules 1994; **27:** 1774.
[50] Yoshizawa H., Chen Y.L. and Israelachvili J.N., J. Phys. Chem. 1993; **97**: 4128.
[51] Yamada S., and Israelachvili J.N., J. Phys. Chem. B 1998; **102:** 234.
[52] Packham D.E., Int. J. Adhesion Adhesives 1996; **16:** 121.
[53] Bhushan, B., Israelachvili J.N and Landman, U., Nature 1995; 374:607
[54] Evans J.R.G. and Packham D.E., J. Adhesion 1979;10:177.
[55] Mecholsky, J.J., Proc. XVII Int. Congress on Glass, vol. 5, p. 473, Chinese Ceramic Society, Beijing, 1995.